COMBINED SENSOR NOISE IMMUNITY IN DIFFUSIVE AND COHERENT FIELDS

PACS REFERENCE: 43.30

Vladimir A. Shchurov
Pacific Oceanological Institute 43, Baltiyskaya St,
Vladivostok, Russia, 690041
E-mail: shchurov@poi.dvo.ru

INTRODUCTION

Combined sensor is the key element of systems designed for acoustic intensity measurements. Combined sensor is composed of a pressure (scalar) sensor and a three-component particle velocity or particle acceleration (vector) sensor. Today betterment of single combined sensor characteristics as well as improvement arrays thereof remain very topical problem. Extensive studies of single combined sensor noise-immunity have been done by many groups. However, in most theoretical papers the combined sensor noise-immunity is solely treated in terms of directional properties of the separate channel dipole characteristics while doing additive or multiplicative processing of acoustic data [1,2]. A lot of papers present the results from mathematical simulation (e.g., see Refs. 3 and 4). Combined sensor noise-immunity estimation on the basis of measurements collected in the actual noise field is a special topical problem today. The paper discusses a multiplicative processing of the four-component combined sensor data. Theoretical part of the paper derives an equation for signal–to–noise ratio (SNR) and introduces a combined sensor gain for multiplicative processing in narrow frequency band. An analysis of the combined sensor noise-immunity for narrow frequency band has been performed using dynamic noise measurements done in deep open ocean. Hence, the paper may be considered as an attempt to interpret specific experimental data in the framework of simple mathematical model in spectral space, likewise well-known similar procedure developed for hydrophone array data processing (see [7]). The approach proposed here for the intensity vector measurement was not applied before by any other author.

COMBINED SENSOR GAIN STUDYING IN FREQUENCY SPECTRA

Suppose both signal and noise (pressure $P(t)$ and a three – component particle velocity $V_x(t)$, $V_y(t)$, $V_z(t)$) to be statistically independent stationary Gaussian processes with zeroth means. Using [5,6] one can write down the single combined sensor signal-to-noise ratio $SNR(PV)$ for multiplicative data processing as:

$$SNR(PV) = \sqrt{\frac{B_0 T_0}{2}} \times \frac{S_{P,S}(f_0) S_{V,S}(f_0) \cos \varphi_S}{S_{P,N}(f_0) S_{V,N}(f_0) \cos \varphi_N} \quad . \qquad (1)$$

Quantities $S_{P,S}(f_0)S_{V,S}(f_0)\cos \varphi_S = S_{PV,S}(f_0)$ and $S_{P,N}(f_0)S_{V,N}(f_0)\cos \varphi_N = S_{PV,N}(f_0)$ represent real parts of the cross spectra for the signal and noise at f_0 and 1-Hz frequency bin. Eq. 1 in logarithmical form is

$$SNR(PV) = 10\lg\sqrt{\frac{B_0 T_0}{2}} \times \frac{S_{PV,S}(f_0)}{S_{PV,N}(f_0)}. \quad (2)$$

SNR(P²) for a single hydrophone (quadratic detector) as

$$SNR(P^2) = 10\lg\sqrt{\frac{B_0 T_0}{2}} \times \frac{S_{P^2,S}(f_0)}{S_{P^2,N}(f_0)}, \quad (3)$$

where $S_{P^2,S}(f_0)$ and $S_{P^2,N}(f_0)$ are the potential energy density spectra of the signal and noise for 1-Hz frequency bin at f_0.

The combined sensor noise-immunity compared with quadratic detector:

$$SNR\left(PV/P^2\right) = \frac{SNR(PV)}{SNR(P^2)}. \quad (4)$$

Eqs. 2 and 4 are very convenient while studying the combined sensor noise-immunity in the narrow frequency band in spectral space.

Replace cross-spectral densities $S_{PV,S}(f_0)$ and $S_{PV,N}(f_0)$ with coherent power of signal and noise: $S_{PV,S}(f_0) = g^2_{PV,S}(f_0) S_{P^2,S}(f_0)$; $S_{PV,N}(f_0) = g^2_{PV,N}(f_0) S_{P^2,N}(f_0)$, where $g^2_{PV,S}(f_0)$ and $g^2_{PV,N}(f_0)$ are simple single-point coherence functions for the signal and noise respectively; $S_{P^2,S}(f_0)$ and $S_{P^2,N}(f_0)$ are auto-power spectrum densities for the signal and noise respectively, so:

$$SNR(PV) = 10\lg\sqrt{\frac{B_0 T_0}{2}} \times \frac{g^2_{PV,S}(f_0) S_{P^2,S}(f_0)}{g^2_{PV,N}(f_0) S_{p^2,N}(f_0)} = 10\lg\frac{S_{p^2,S}(f_0)}{S_{p^2,N}(f_0)} + 10\lg\sqrt{\frac{B_0 T_0}{2}} \times \frac{g^2_{PV,S}(f_0)}{g^2_{PV,N}(f_0)}. \quad (5)$$

The term $10\lg\frac{S_{p^2,S}(f_0)}{S_{p^2,N}(f_0)}$ in Eq. 5 is equal to *SNR(P²)* at the output of hydrophone incorporated in combined sensor. The following equation

$$k = 10\lg\sqrt{\frac{B_0 T_0}{2}} \times \frac{g^2_{PV,S}(f_0)}{g^2_{PV,N}(f_0)} \quad (6)$$

is equal to the expression for N-element antenna array gain 10lgN referred to in [7], so, following Ref. 7 it would be reasonable to call k as combined sensor gain. Hence, the combined sensor gain depends on the ratio between the noise and signal coherence functions $g^2_{PV,S}(f_0)$, $g^2_{PV,N}(f_0)$ as well as frequency band width B_0 and average time T_0.

SPECIAL FEATURES OF COMBINED SENSOR SNR FORMING IN THE ACTUAL OCEAN NOISE FIELD FOR NARROW FREQUENCY BAND

A behavior of 622-Hz fluctuating tone was studied. Time series 1800 s long were used. The experiment conditions were as follows, 4000-m deep water, axis of the underwater sound channel at the depth of 1200 m, near-surface wind speed of 6 to 7 m/s, well-developed wind-generated surface roughness, swell. Operating modules with combined sensors were centered at two depths, 150 and 300 m, *x*-and *y*-axes of both combined sensors were lying in the horizontal plane, *z*-axis is directed downward. The tone source was at the depth of 100 m 4 to 6 km apart from the measurement system. During the experiment fluctuating signal level in pressure auto-spectrum exceeded the noise spectrum level by less than 6 dB for the combined sensor centered at 150 m. *X*- and *y*-axes are arranged in the ocean waveguide so that horizontal projection of the energy flux in the dynamic noise coherent field $I_{+x,N}$ is aligned with +*x*-axis; the signal energy flux projection $I_{-x,S}$ is aligned with –*x*-axis; the energy flux from the local source $I_{-y,S}$ is aligned with –*y*-direction; at 622 Hz the dynamic noise field in *y*-direction is diffusive. Dynamic noise energy flux projection $I_{+z,N}$ is aligned with +*z*-axis; opposite projection of the signal energy flux $I_{-z,S}$ is, naturally, aligned with –*z*-axis. The research vessel remained drifting during the whole experiment. When the drifting vessel was sharp on *y*-axis of the combined receiver, a response to the sound source signal at the *x*-channel output vanished. In the vertical plane energy fluxes $I_{-z,S}$ and $I_{+z,N}$ compensated one another [5,6,9,10].

Combined Sensor Gain in the Dynamic Noise with Prevailing Diffusive Component

Measurements from two time series (one from the depth of 150 m, the other from 300 m) 1800 s long each at central frequency f_0=622 Hz were used in studying combined sensor SNR discussed in the paper. Signal-to-noise ratio was calculated from Eqs. 2 and 3 via corresponding spectral densities for the following quantities: 1. potential energy density spectrum $SNR(P^2)$; 2. *y*-projection of the kinetic energy density spectrum $SNR(V^2_y)$; 3. *y*-projection of the energy flux density spectrum $SNR(PV_y)$.
Exponent averaging over the following periods $Ò_0$= 1; 1.4; 2; 5; 15; 30; 45; 60; 64; 75; 90; 100; 110; 150; 192; 200; 250; 300; 320 s has been done Frequency band of analysis was 1Hz. Mean values $<SNR(P^2)>$, $<SNR(V^2_y)>$, $<SNR(PV_y)>$ were also calculated for each average time $Ò_0$. Average-time-dependence curves $<SNR(P^2)>$, $<SNR(V^2_y)>$, $<SNR(PV_y)>$ over the whole time series 1800 s long are shown in Figs. 1a,b (for 150-m and 300-m measurement depths respectively). As seen from Figs. 1a,b both $<SNR(P^2)>$ and $<SNR(V^2_y)>$ reach their maximums when T_0 reaches its critical value $T_c \approx 5$ s and further remain independent of average time. Plausible estimates are as follows: at 150 m $<SNR(P^2)> = 3.5$ dB, $<SNR(V^2_y)> = 7.3$ dB (the difference in level is 3.8 dB); at 300 m $<SNR(P^2)> = 6.6$ dB, $<SNR(V^2_y)> = 11.2$ dB (the difference in level is 4.6 dB). The level difference between $<SNR(P^2)>$ and $<SNR(V^2_y)>$may be attributed to dipole directivity pattern of particle velocity sensor channel whose directivity factor is 3. Consequently, in pure isotropic noise field $SNR(V^2_y)$ should be greater than $SNR(P^2)$ by 4.8 dB. Deviation from this value indicates anisotropic component existing in ambient noise field. For the depth of 150 m deviation is 1dB; at the same time for the depth of 300 m that is 0.2 dB. Consequently, the field at 150 m is less isotropic in the horizontal plane than at 300 m, namely, the isotropic field contribution representing 79% of the total noise energy density at 150 m, runs up to 95% at the 300-m depth. $<SNR(PV_y)>$ depends on T_0 until $T_0 \le T_c$ and becomes practically independent of average time at $T_0 > T_c$. Function $(a+â\sqrt{T})$ has been constructed to approximate $<SNR(PV_y)>$ (Figs. 1a,b). The approximation has the following coefficients: 1) for the depth of 150 m a=12.8, b=7.7 $s^{-1/2}$; average times used T_0 = 1.4; 2; 5; 15; 30; 45; 60; 64; 75; 90; 100; 110; 150 s; 2) for the depth of 300 m a=37.5, b=17.5 $s^{-1/2}$. Corresponding average times, T_0=1.4; 2; 5; 15; 30; 45; 60 s. Approximation $(a+â\sqrt{T})$ coincide with the experimental data $<SNR(PV_y)>$ until $T_0 \le T_c \approx 120$ s for 150 m and until $T_0 \le T_c \approx 60$ s for 300 m. As noted above, one should take average time of about 5s to obtain the maximums of both $<SNR(P^2)>$ and $<SNR(V^2_y)>$, on the other hand, to achieve the maximum of $<SNR(PV_y)>$ $T_c \approx$ 60-120 s is required. Hence, to obtain the maximum of $<SNR(PV_y)>$ one should average data over a period 12-24 times greater than that required for maximum $<SNR(P^2)>$ or $<SNR(V^2_y)>$. In doing so the excess of the combined sensor noise-immunity over that of the quadratic detector is $SNR(PV_y / P^2) = <SNR(PV_y)> - <SNR(P^2)> \approx 15 - 16$ dB (Figs. 1a,b). As follows from Fig. 1, experimental data agree with the approximation $a+â\sqrt{T}$ for $Ò_0 \le Ò_c$.

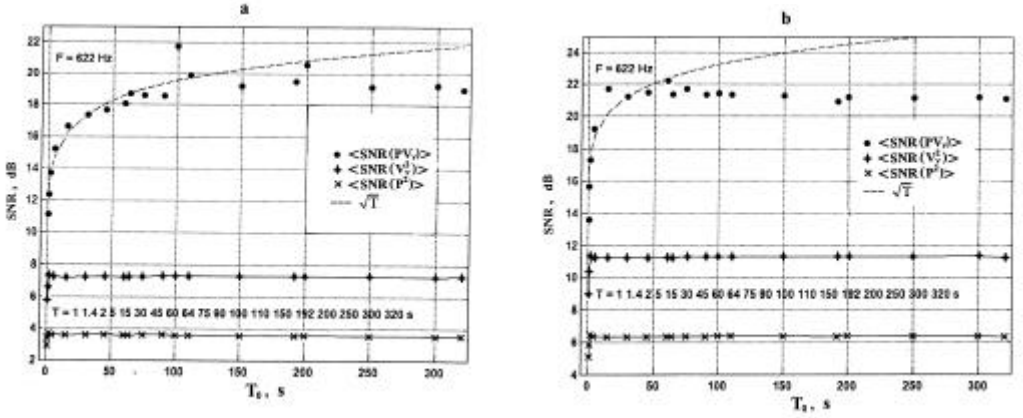

Figure 1. The average-time-dependence of $<SNR(P^2)>$, $<SNR(V^2_y)>$, $<SNR(PV_y)>$. Measurement depth is a) 150 m, b) 300 m. Approximation $(à + â\sqrt{Ò})$ is plotted with a dashed line; $Â_0$ = 1 Hz.

Coherent Properties of Signal and Noise Energy Fluxes

Consider dependence of noise and signal coherent properties on average time T_0 for the data collected at 150-m depth. Use the same time series 1800 s long as in Section 3.1. Exponent averaging over the following times T_0 = 3; 5; 15; 30; 45; 60; 75; 90; 100; 150; 192; 200; 250; 300; 320 s was performed. Study behavior of the combined sensor gain k. Fig. 2 shows noise and signal coherence functions $\gamma^2_{PV_y,N}(f_0)$ and $\gamma^2_{PV_y,S}(f_0)$ for above-mentioned time series 1800 s long at f_0 =622 Hz and three average times T_0 = 5; 15; 30 s. As follows from Fig. 2, the 622-Hz signal coherence function fluctuates in time whereas the noise coherence function remains constant (for each T_0) and decreases with increasing average time.

Fig. 3 shows average-time-dependence of the noise coherence function $\gamma^2_{PV_y,N}(f_0)$ along with the corresponding standard deviation $\sigma_N(f_0)$ as well as average-time-dependence of the signal coherence function $\gamma^2_{PV_y,S}(f_0)$ along with the corresponding standard deviation $\sigma_S(f_0)$. $\gamma^2_{PV_y,S}(f_0)$ and $\sigma_S(f_0)$ were calculated using two intervals from the same time series, t_1= 700-800 s (Fig. 3b) and t_2 = 1200-1500 s (Fig. 3c). Noise coherence decreases with increasing average time (Fig. 3a). For T_0=3 s $\gamma^2_{PV_y,N}(f_0)\pm\sigma_N(f_0)$=0.415±0.021; for T_0=320 s $\gamma^2_{PV_y,N}(f_0)\pm\sigma_N(f_0)$=0.008±0.003, i.e. the coherence level drops by 17 dB. In doing so the standard deviation $\sigma_N(f_0)$ decreases by about 8.5 dB (from 0.021 down to 0.003). Hence, in y direction diffusive component of the noise prevails. While increasing average time the signal coherence initially decreases and then remains constant until T_0=320 s (Fig. 3b,c).

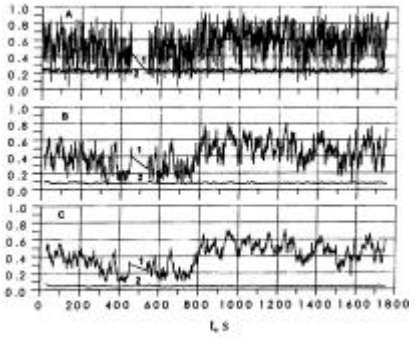

Figure 2. (1) - signal coherence function $\gamma^2_{PV_y,S}(f_0)$, (2) - noise coherence function $\gamma^2_{PV_y,N}(f_0)$ for f_0 = 622 Hz. Average time for each spectrum: À –5 s, Â – 15 s, Ñ – 30 s, band of the analysis is 1Hz. During the period 450 to 510 s the combined sensor is turned off due to a pause in the telemetric system radio-cannel operation.

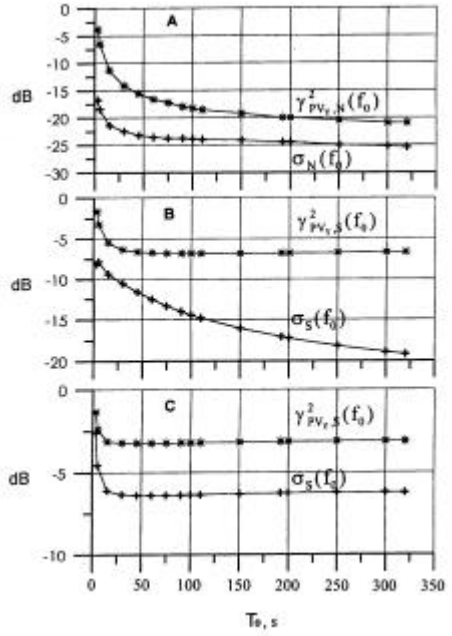

Figure 3. Dependence of $\gamma^2_{PV_y,N}(f_0)$, $\sigma_N(f_0)$ and $\gamma^2_{PV_y,S}(f_0)$, $\sigma_S(f_0)$ on average time T_0. 0dB level corresponds to the maximum value of the coherence function that is unity.

In the case of weak signal the signal coherence decreases until T_0=30 s (Fig. 3b), at the same time its standard deviation $\sigma_S(f_0)$ decreases with increasing average time. For more strong signal the coherence decreases until T_0=15 s (Fig. 3c) and then remains constant with corresponding standard deviation decreasing until T_0=15 s and then coming constant. As follows from Fig. 3 the signal coherence is constant for average times greater than 30 s, on the other hand the noise coherence decreases as well as its standard deviation when T_0 increases. It is apparent that the combined sensor gain k has to grow with average time. Fig. 4 shows the dependence of the combined sensor gain on T_0 for two intervals, t_1=700-800 s and t_2=1200-1500 s (with constant excess of the signal over the noise

in each interval). Marks ▲ and + are used to denote experimental data. Approximation functions $à + â\sqrt{Ò}$ (for $Â_0$ = 1 Hz) are plotted with solid lines. Fig. 4 illustrates that <k> depends on $Ò_0$ the same way as <*SNR(PV$_y$)*> does (re Fig. 1a.).

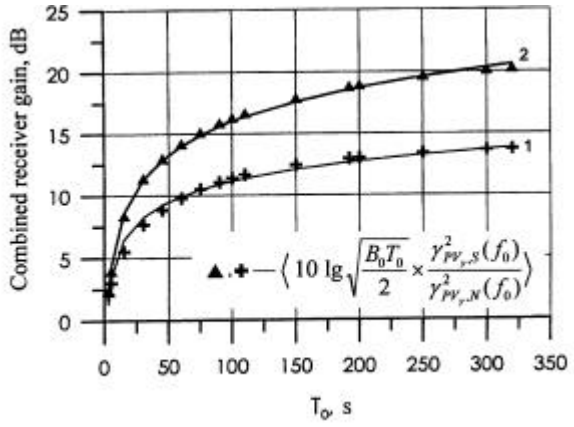

Figure 4. The dependence of the combined sensor gain on the averaging time $Ò_0$. Measurement depth is 150 m. Marks "+" correspond to the time period 700 –800 s, whereas marks "▲" correspond to the time period 1200 to 1500 s in Fig. 2. Approximation curves *(à + $â\sqrt{Ò}$)* are plotted with solid lines 1 and 2; $Â_0$= 1 Hz.

Combined Sensor Signal-to-Noise Ratio SNR(PV) in Coherent Noise Field Under Signal/Noise Compensation Condition

While passing in opposite directions noise and signal energy fluxes may result in zeroth net flux. The phenomenon has been observed a number of times at many deployment sites in deep and shallow water and referred to as compensation [9,10], which may be used to detect a signal against the noise background [5,6]. Hydrophone antenna arrays are incapable of registrating phenomenon of compensation, consequently, this approach to the signal detection is peculiar to combined sensors. Naturally, mutual compensation of two weak opposite noise and signal energy density fluxes is the most interesting occasion. In the given case compensation between vertical projection of the signal energy flux reflected from the bottom and opposite ambient noise energy flux transporting the dynamic noise energy downward to the bottom was exhibited. Consider *SNR(PV$_z$)* for the vertical projection of the fluctuating tone energy flux under compensation condition. The following designations used: vertical projection of the noise energy flux spectral density coming in+z direction $S_{PVz,N}(f_0)$; vertical projection of the signal energy flux spectral density coming in *–z* direction $S_{PVz,S}(f_0)$. Define *SNR(PV$_z$)* as a ratio between $S_{PVz,N}(f_0)$-$S_{PVz,S}(f_0)$, (net flux in z direction) and the noise level $S_{PVz,N}(f_0)$:

$$SNR(PV_Z) = 10\lg \frac{S_{PVz,N}(f_0) - S_{PVz,S}(f_0)}{S_{PVz,N}(f_0)} = 10\lg\left(1 - \frac{S_{PVz,S}(f_0)}{S_{PVz,N}(f_0)}\right). \qquad (7)$$

In idealized limiting case of full compensation $\{(S_{PVz,S}(f_0))/(S_{PVz,N}(f_0))\} \to 1$, and $SNR(PV_z) \to -\infty$. With no signal $S_{PVz,S}(f_0)=0$ and $SNR(PV_z)=0$. That is, *SNR(PV$_z$)* is universally negative when opposite energy fluxes compensation exists. Consider an example of compensation at a frequency of the tone signal f_0=622 Hz. Fig. 5 shows spectral levels $S_{p^2}(f)$ and $S_{PVz}(f)$ (time of exponent averaging is 30 s, frequency bin is 1.5 Hz). The notch in $S_{PVz}(f)$ spectrum is 30 dB deep, i.e. $SNR(PV_z)$=-30 dB. Physically, the notch in $S_{PVz}(f)$ means that in 1.5-Hz surrounding of

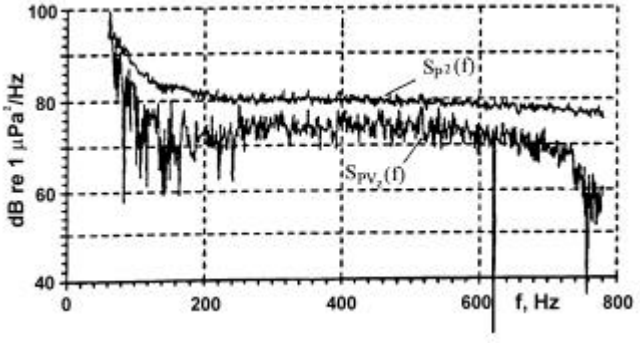

Figure 5. Ambient noise spectral densities, $S_{p^2}(f)$, $S_{PV_z}(f)$. The notch at f_0 = 622 Hz results from the compensation of opposite noise and tone energy fluxes. Exponent averaging over 30 s. Measurement depth is 150 m, wind speed is 7 m/s.

622 Hz net energy flux through the unit surface placed orthogonal to *z*-axis at the measurement point is 10^3 times (by 30 dB) less than the ambient noise energy flux existing with no signal.
Hence, the notch at f_0 = 622 Hz indicates that just a weak signal exists along with the ambient noise since just a little part of the noise energy flux has been compensated up.
As experimentally shown in Refs. 9-10, broadband noise-like signals whose spectra $S_{P^2,S}(f)$ are similar to ambient noise spectra $S_{P^2,N}(f)$, are also detectable under compensation condition.

CONCLUSIONS

Expression for *SNR(PV)* for a single combined sensor has been theoretically derived and the combined sensor gain has been introduced for multiplicative data processing for both wide and narrow frequency bands.
Statistical data processing evidences that standard deviation of the horizontal projection of the dynamic noise energy flux density falls off with increasing average time as $1/\sqrt{T_0}$ ($\hat{A}_0$ = 1 Hz) until the average time reaches its critical value $\tau_0=\tau_c$. To obtain a reliable estimation of $SNR(PV_y)$ one should average data over a period τ_c, 12 to 24 times greater than that required for reliable estimations of $SNR(P^2)$ or $SNR(V^2_y)$ for the potential and kinetic energy densities respectively.
Verification of theoretically-derived $SNR(PV_y)$ and $SNR(PV_z)$ on the base of recording of fluctuating tone on underwater dynamic noise background in deep ocean have been done.
As follows from the experimental estimation made, the maximum excess of SNR of combined sensor measuring the energy flux density over SNR of hydrophone measuring the potential energy density is 15 to 16 dB for the horizontal energy flux density projection and may run up to 30 dB for the vertical one under signal/noise energy fluxes compensation condition.

REFERENCES

1. Smaryshev M.D., Shenderov E.L. Noise-immunity of plane arrays in anisotropic noise field.//Akusticheski. Journal. (in Russian), 1985, V.31, ¹ 4: P. 502–506.
2. Gordienko V.A., Ilyichev V.I., Zakharov L.N. Vector-phase technique in acoustics (in Russian). Nauka, Moscow; 1989: 223 p.
3. Dorodnova I.A., Olshevski V.V. Characteristics of detection of hydroacoustic signals against the noise background while using combined sensors, models and algorithms developed for acoustic data processing systems.// Sbornik nauchnyh trudov LIAP (in Russian), Ed. by Ilyichev V.I. and Lukoshkin A.P., Leningrad, 1990; P.112–117.
4. Pasechnyi S.V. Comparison evaluation between noise-immunity of plane arrays and linear combined antennas in the waveguide.// Naychnye trudy *LIAP*, Ed. by Ilyichev V.I. and Lukoshkin A.P. Leningrad, 1990; P. 106 – 112.
5. Shchurov V.A. and Shchurov A.V., Noise Immunity of a Combined Reseiver Hydroacoustic.// Akustiticheskii Journal (in Russian) 2002; V. 48, ¹ 1. P. 110-119.
6. Shchurov V.A., Shchurov A.V., Combined sensor noise-immunity.// Chinese Journal of Acoustics, 2002.
7. Burdic W.S. Underwater acoustic system analysis. Prentice-Hall, INC. N-Y 07632:1984: 391p.
8. Shchurov V.A. Kuyanova M.V., Use of acoustic intensity measurements in underwater acoustics (Modern state and prospects)// Chinese Journal of Acoustics, 1999. V.18. ¹ 4. P. 315-326.
9. Shchurov V.A., Ilyichev V.I., Kouleshov V.P., Kuyanova M.V. “The interaction of energy flows of underwater noise and a local source.// J. Acoust. Soc. Am., 1991; ¹ 90 (2): P. 1002–1004.
10. Shchurov V.A., Ilyichev V.I. The properties of the vertical and horizontal power flows of the underwater ambient noise.// Natural physical sources of underwater sound, Ed. by B.R.Kerman, Kluwer Academic Publishers, Netherlands, 1993; P. 93-109.